A&A 581, A26 (2015)
DOI: 10.1051/0004-6361/201526059


Astronomy & Astrophysics

# Hydrogen Ly-$\alpha$ and Ly-$\beta$ full Sun line profiles observed with SUMER/SOHO (1996–2009)⋆

P. Lemaire[1], J.-C. Vial[1], W. Curdt[2], U. Schühle[2], and K. Wilhelm[2]

[1] Institut d'Astrophysique Spatiale (IAS), Unité mixte CNRS-Université, Université Paris XI, bât.121, 91405 Orsay, France
e-mail: lemaire@ias.u-psud.fr
[2] Max-Planck-Institut für Sonnensystemforschung, Justus von-Leibig-Weg 3, 37077 Göttingen, Germany

Received 9 March 2015 / Accepted 19 June 2015

**ABSTRACT**

*Context.* Accurate hydrogen spectra emitted by the entire solar disc in the Ly-$\alpha$ and Ly-$\beta$ lines are valuable for deriving the distribution and the behaviour of atomic hydrogen in the heliosphere, for understanding the UV emissions of solar type stars better, and finally for estimating the solar energy input that mainly initiates the chemical processes occurring in the planetary and cometary outer atmospheres.
*Aims.* In this paper we want to accurately determine the irradiance solar spectral profiles of Ly-$\alpha$ and Ly-$\beta$ and their evolution through the solar activity cycle 23.
*Methods.* The SUMER/SOHO spectrometer is a slit spectrometer that is only able to analyse a small part of the solar image. Consequently, we used the scattered light properties of the telescope to obtain average spectra over the solar disc. Then the profile is calibrated using the SOLSTICE/UARS and TIMED/SEE irradiance spectra.
*Results.* We obtained a set of irradiance Ly-$\alpha$ and Ly-$\beta$ solar spectra with a 0.002 nm resolution through the solar activity cycle 23. In each line a relation between the integrated profile and the line centre intensity was obtained.Knowing the line irradiance, it is possible to deduce the central line profile intensity, a critical input into the interplanetary and planetary oxygen and hydrogen fluorescent processes.
*Conclusions.* The observation of H I Ly-$\alpha$ and Ly-$\beta$ line profiles by SUMER/SOHO during the cycle 23 allows analysis of the evolution of their characteristics and accurate determination of UV radiation input into the solar system.

**Key words.** Sun: chromosphere – Sun: UV radiation – Sun: heliosphere

## 1. Introduction

Having been produced by the most abundant element in the low solar atmosphere, the resonance solar H Ly-$\alpha$ line (121.567 nm) is the most prominent emission feature in the solar ultraviolet spectrum. Knowing the full Sun H Ly-$\alpha$ line profile is then essential for investigating several astrophysical questions. For example, it constrains the energy budget of the solar atmospheric models and then provides a standard for modelling the atmospheres of solar type stars. The solar H Ly-$\alpha$ line is also the main source of resonant excitation of the hydrogen present in the planetary and cometary atmospheres and/or exospheres, as well as the heliosphere (Nina & Cadez 2014; Bzowski et al. 2013).

Similarly, the Ly-$\beta$ line (102.572 nm) provides complementary constraints on the solar atmospheric models. The line profile is used to determine the fluorescence rate of the O I through the pumping process of the O I 102.577 nm line in the solar atmosphere (Haisch et al. 1977) and also in comets (Feldman et al. 1976).

Previously the high resolution spectral irradiance (full-disc) Ly-$\alpha$ and Ly-$\beta$ profiles at solar minimum (beginning of solar cycle 21) have been obtained (Lemaire et al. 1978) using data from the OSO8/LPSP multi-channel spectrometer instrument. More recently, the variation in the solar spectral irradiance Ly-$\alpha$ and Ly-$\beta$ profiles over the beginning of solar cycle 23 using the SOHO/SUMER spectrometer has been reported (Lemaire et al. 1998, 2005). The uniqueness of the SUMER/SOHO Ly-$\alpha$ and Ly-$\beta$ profiles taken at the $L_1$ Lagrangian position (between Sun and Earth) is that they are free of any geocoronal absorption in the central core of the lines.

The present paper analyses the variation in the irradiance Ly-$\alpha$ and Ly-$\beta$ profiles over the full solar cycle 23 (1996–2009) and gives the relations between the irradiance at the Ly-$\alpha$ and Ly-$\beta$ line centres and the full (spectral integral) lines.

## 2. Observations

### 2.1. SUMER scattering properties

The SUMER spectrometer is described in Wilhelm et al. (1995), and its in-flight performances are reported in Lemaire et al. (1997) and Wilhelm et al. (1997). The spectral resolution is limited by the two-pixel sampling rule (i.e. 2 × 0.0043 nm near 121 nm and 2 × 0.0044 nm near 102 nm) with the 1 arcsec-entrance slit width.

We used the scattering properties of the telescope that average the details over the disc to build the spectral profiles integrated over the solar disc. The telescope point spread function (PSF) was established before assembly of the instrument. The PSF core was published in Lemaire et al. (1997), and the PSF tail (up to 50 arcmin) was reported in Saha et al. (1996).

⋆ Profiles are only available at the CDS via anonymous ftp to cdsarc.u-strasbg.fr (130.79.128.5) or via http://cdsarc.u-strasbg.fr/viz-bin/qcat?J/A+A/581/A26

The measured scattered light at some given distance from the solar disc is the result of the convolution of the PSF with the observed disc brightness (see 3.3).

Lemaire et al. (1998) provides more details on the averaging process over the solar disc using the measurement of the scattered light at off-limb positions.

### 2.2. Observations

Most of the observations reported in this paper have been taken with the $1'' \times 300''$ slit at two opposite off-limb positions above and below the solar equator ($Y$ axis along the south-north polar axis and parallel to the slit) in order to improve the averaging given by the scattered light. They were recorded over several hours to increase the signal-to-noise ratio. The parameters of each observation taken between 1996 and 2009 are presented in Tables A.1 and A.2. The main parameters are:

- the start time of exposures (date and time) with a four-hour total duration at each one- or two-slit position (in $+Y$ and in $-Y$) and a two-hour duration at each four-slit position in 1996 ($\pm X$ and $\pm Y$);
- the slit location with the $1'' \times 300''$ slit size;
- the detector (A or B) used;
- the Ly-$\alpha$ irradiance taken from *composite_lya.dat* (http://lasp.colorado.edu/lisird, Woods et al. 2000);
- the 10.7 cm radio flux from *Solar Indices Bulletin* (National Geophysical Data Center, STP Division).

## 3. Data reduction

### 3.1. Average raw profile

For each set of observations, the data are pre-processed following the SUMER standard procedure (decompression, flat field, and distortion correction) for each detector image. Then detector images taken at the same location are magnified throughout the spectral domain (by a factor 8 for Ly-$\alpha$ and factor 4 for Ly-$\beta$). Along the slit image, where the pixel size corresponds to ~1 arcsec, the detector is subdivided in six sets of 40 spectra (avoiding the slit-image edges). The spectra of each set are co-aligned, added and normalized to 1 arcsec (i.e. ~1 pixel) and 1 s exposure. Then the centre of gravity of each average spectrum is determined and the spectral result shifted and aligned with the first average spectrum. This results in six average spectra for each pointing position. By using reference lines (see Sect. 4) each spectrum is calibrated in wavelength, and the counts number is normalized in units of angular pixel (arcsec) and time exposure (s).

### 3.2. Normalization at 800″ above solar limb

Each observation has been taken at a defined location (not always at the same distance from the solar limb) and at different times (with different solar conditions). The level of the measured scattered light depends on the distance from the solar limb and the distribution of solar features on the disc and their variation. To compare all the profiles we need to refer to the same distance from the limb, and the 800″ off-limb was selected as the reference.

First, the Lyman solar disc distribution for the date of observation is established. To obtain this distribution, the EIT 30.4 nm solar image (Delaboudiniére et al. 1995) corresponding to the time of observation is used and weighted by the ratio H I Ly-$\alpha$ (or $\beta$) to He II 30.4 (Vernazza & Reeves 1978; Auchère 2005).

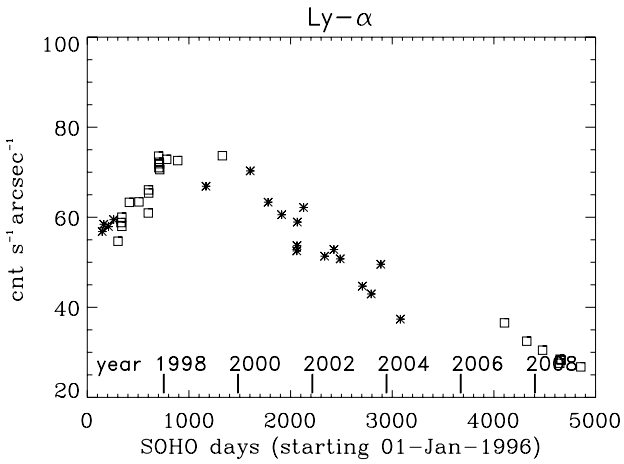


**Fig. 1.** Total number of scattered light counts in the Ly-$\alpha$ line normalized at 800″ off-limb on the KBr part of the detectors; * for detector A and squares for B.

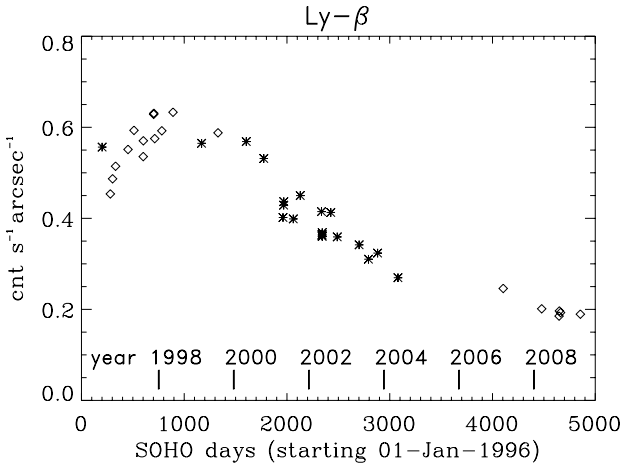


**Fig. 2.** Total number of scattered light counts in the Ly-$\beta$ line normalized at 800″ off-limb on the KBr part of the detectors; * for detector A and diamonds for B.

Then, the coordinates of each section of the slit (6 sections) are computed and the convolution of the solar disc intensity by the PSF profile gives the relative scattered light contribution at this location compared to the 800″ reference distance from the solar limb. All the data from the same set of observations are added, normalized to one second and one arc second at the 800″ off-limb distance. Now the set of data (in counts per second and arcsecond) only depends on the solar activity and on the long-term change in the spectrometer sensitivity (see Figs. 1 and 2).

### 3.3. The relative telescope scattered light accuracy

The two curves displayed in Fig. 3 show the distribution of the scattered light above the limb for the maximum and the minimum of the solar activity cycle 23. Here, the discrepancy between the two curves is very small.

In the same figure we have superposed the data points obtained from all observations (6 positions along the 300 arcsec slit). Each observation was fitted by a scattering curve, and each curve was shifted to coincide with the same value

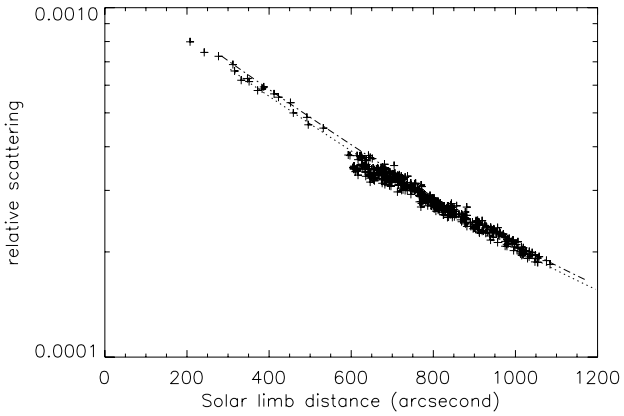


**Fig. 3.** Telescope scattered light at 121.6 nm from data obtained during the 1996–2009 period (+ are the measured data, -.- and ... are the estimate scattered curves for July 1996 and October 2001; min/max solar activity of cycle 23.

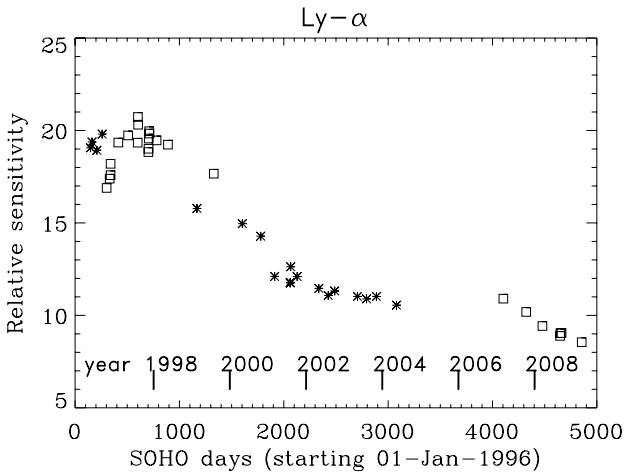


**Fig. 4.** Ly-$\alpha$ relative variation of responsivity on the KBr part of the detectors; * for detector A and square for B.

at 800 arcsec off-limb. The dispersion provides an estimate of the measurement accuracy (±6%).

## 4. Calibrations and profiles

### *4.1. Ly-α*

#### 4.1.1. Ly-α calibration

The chromospheric/transition region lines (Si III 120.6499 nm, O V 121.8393 nm and Mg X 60.9794 × 2 nm (second grating order) are used to measure the dispersion and establish the wavelength scale (±0.0015 nm accuracy; see Lemaire et al. 2002). The *composite_lya.dat* (lasp.colorado.edu/lisird, Woods et al. 2000) is used as a reference for absolute irradiance calibration with ±10% estimated accuracy. There are two additional sources of error:

– normalization to 800 arcsec,
– observations are made during a few hours of the day, while the reference flux is averaged daily (cf. *composite_lya.dat*).

The final calibration accuracy is estimated to be ±15%. It is interesting to note that using this reference flux and the data shown in Fig. 1, the time variation of the spectrometer responsivity at 121.6 nm can be established (see Fig. 4).

#### 4.1.2. Ly-α profiles

The calibrated Ly-$\alpha$ irradiance profiles are displayed in Fig. 5a. Using the Richardson-Lucy deconvolution algorithm (which in turn uses the maximum likelihood principle, Waniak 1997) with the telescope PSF, improved Ly-$\alpha$ irradiance profiles are obtained (Fig. 5b). The deconvolution increases the ratio between peaks and core.

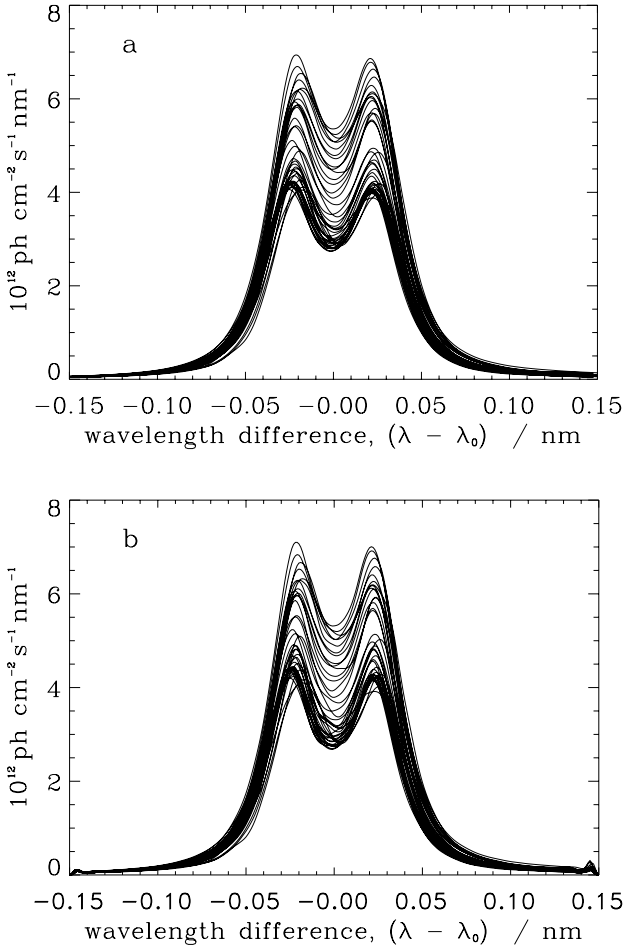


**Fig. 5.** Ly-$\alpha$ spectral line profiles of the photon irradiance during the 1996–2009 years, where $\lambda_0$ is the Ly-$\alpha$ reference wavelength (121.567 nm): **a)** data; **b)** data deconvolved with the SUMER PSF.

### *4.2. Ly-β*

#### 4.2.1. Ly-β calibration

The O I 102.74307 and 102.81571 lines and, when available within the detector frame, C I 103.6336 and 103.7018 lines are used to establish the dispersion and the absolute wavelength scale (±0.002 nm accuracy).

The 121.6/102.5 nm responsivity ratio for A and B detectors was established during calibrations before launch (Wilhelm et al. 1995). Then, because it is near the ecliptic plane and is in the field of the SUMER telescope, several observations of the $\alpha$-Leo star were made to follow the relative responsivity variation of the instrument and were used to measure the 121.6/102.5 nm responsivity ratio (Lemaire 2002). After the beginning of TIMED mission in 2002, the SEE experiment has been providing the referenced Ly-$\beta$ irradiance

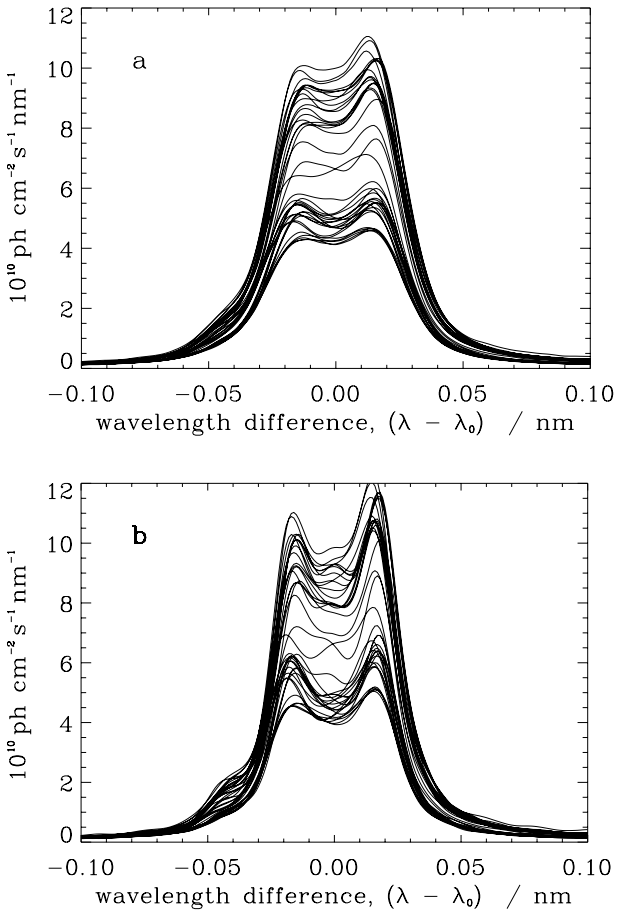


**Fig. 6.** Ly-$\beta$ spectral line profiles of the photon irradiance during the 1996–2009 years, where $\lambda_0$ is the Ly-$\beta$ reference wavelength (102.572 nm): **a)** data; **b)** data deconvolved with the SUMER PSF; the helium He II 102.524 nm line is detected in the blue wing of Ly-$\beta$ (Ebadi et al. 2009).

(Woods et al. 2005). The Ly-$\alpha$/Ly-$\beta$ irradiance relation established in Lemaire et al. (2012) is used to confirm the irradiance calibration (±20% accuracy).

#### 4.2.2. Ly-$\beta$ profiles

The calibrated Ly-$\beta$ profiles are displayed in Fig. 6a. With the same deconvolution scheme used above, the improved Ly-$\beta$ profiles are shown in Fig. 6b. Again, the deconvolution increases the ratio of peak-to-centre intensities, and the helium He II 102.524 nm has been extracted from the blue wing (see Ebadi et al. 2009).

## 5. Results and discussion

### 5.1. Ly-$\alpha$

The profiles displayed in Fig. 5b are available in tabular forms via internet. In all profiles, which are characterized by a central self-reversal, the blue peak is higher than the red peak. There is no clear explanation for this difference (systematic downflows or a combination of up and down flows, see Curdt & Tian 2010). Actually, the same asymmetries were noticed in prominences as early as 1982 (Vial 1982), and they have recently been interpreted with a multi-thread model with stochastic velocities

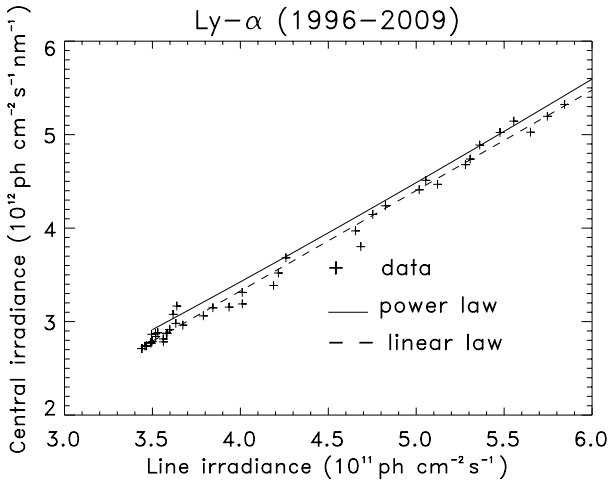


**Fig. 7.** Relation between the central spectral photon irradiance and the total photon irradiance. The power law fit was established by Emerich et al. (2005), and the linear law is from the present paper.

(Gunar et al. 2008). The weak Balmer line of He II (121.513 nm) seen in the blue wing of Ly-$\alpha$ in prominences (Vial et al. 2015) is not detected in the irradiance profile.

To access the Ly-$\alpha$ centre, which excites planetary atmospheres, using OSO-5 data, Vidal-Madjar (1975) computed a first relation between the photon irradiance at the line centre and the same in the full line. This relation was revisited by Emerich et al. (2005) with data obtained by SUMER during the 1996–2003 period (the data have not been deconvolved):

$$f = 0.64\,(F)^{1.21} \pm 0.15$$

with $f = f/(10^{12}$ cm$^{-2}$ s$^{-1}$ nm$^{-1})$, where f is the central spectral photon irradiance and with $F = F/(10^{11}$ cm$^{-2}$ s$^{-1})$, where $F$ is the total Ly-$\alpha$ photon irradiance.

Using the deconvolved Ly-$\alpha$ profiles we improved this result and obtained a linear relation between the centre and the total line:

$$f = -0.968(\pm0.070) + 1.074\ (\pm0.016)F,$$

with $f = f/(10^{12}$ cm$^{-2}$ s$^{-1}$ nm$^{-1})$, where $f$ is the central photon irradiance, and with $F = F/(10^{11}$ cm$^{-2}$ s$^{-1})$, where $F$ is the total photon irradiance. The resulting curve is displayed in Fig. 7.

### 5.2. Ly-$\beta$

The profiles displayed in Fig. 6b are available in tabular forms via internet. In contrast to Ly-$\alpha$ profiles, the red peaks of Ly-$\beta$ profiles are higher than the blue peaks. This has also been observed in the quiet Sun (Tian et al. 2009) and may be explain by an asymmetry between up-flows and down-flows. The basic process at work is the opacity ratio of the Ly-$\alpha$ and Ly-$\beta$ lines, which allows a differential sounding of different layers with varying velocities. One can wonder whether the same process is at work in the solar chromosphere.

The Ly-$\beta$ line centre excites the O I 102.577 solar and planetary atmospheric lines that populate other O I lines by cascades. The relation between the line centre and the full line is given by $f = -0.248\ (\pm0.243) + 1.482\ (\pm0.048)\ F$,

with $f = f/(10^{10}$ cm$^{-2}$ s$^{-1}$ nm$^{-1})$, where $f$ is the central photon irradiance, and $F = F/(10^{9}$ cm$^{-2}$ s$^{-1})$, where $F$ is the total photon irradiance. The resulting curve is displayed in Fig. 8.

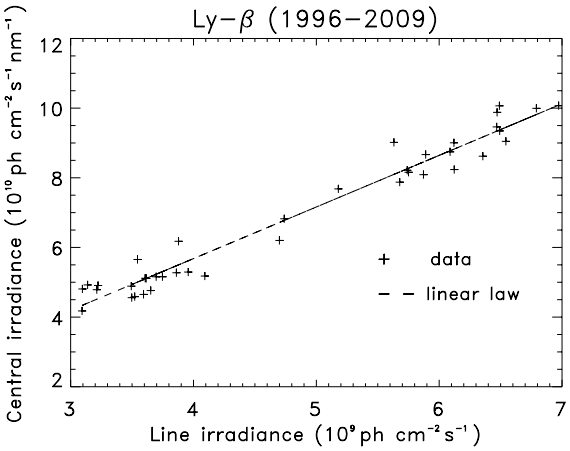


**Fig. 8.** Relation between the central spectral photon irradiance and the total photon irradiance in the Ly-$\beta$ line.

## 6. Conclusions

Using the scattering properties of the SUMER telescope, we have built spectral irradiance H I Ly-$\alpha$ and Ly-$\beta$ profiles through a full solar activity cycle. It is the first time that detailed solar irradiance profiles of H I Ly-$\alpha$ and Ly-$\beta$ have been obtained through the full solar cycle 23. A new relation between the core and the total profile of Ly-$\alpha$ irradiance was computed, and for the first time, a relation between the core and the total profile of Ly-$\beta$ irradiance was obtained.

These results will help to improve the solar/stellar chromospheric models and provide the input flux in planetary and cometary atmospheric modelling. As far as the planetary and cometary observations are concerned, previous observations of Jupiter and Saturn's aurorae with the *Hubble* Telescope (Nichols et al. 2007) and comets (e.g. Bertaux et al. 1973) can be interpreted and modelled with the new relationships. New planetary and cometary observations could be planned with EUI and METIS on Solar Orbiter.

The Lyman-$\alpha$ absorption from hydrogen escaping hot Jupiter exoplanets has recently received much attention (e.g. Bourrier et al. 2013) and requires knowing the incident stellar profile (a K star in the example above) well. The same is true for mini-Neptune atmospheres around M stars (Miguel et al. 2015). The Jovian dayglow has been observed well in Ly-$\alpha$ (e.g. Emerich et al. 2005), and it has been recently modelled for the Ly-$\beta$ line (see Barthélémy et al. 2004, who show that spectral resolution is necessary for separating the central Ly-$\beta$ emission from the H2(6-0 P(1)) emission located 0.021 nm farther). We also mention that routine observations are performed by SWAN/SOHO in the Ly-$\alpha$ line, from which water production rates are derived (e.g. Bertaux et al. 2014).

*Acknowledgements.* SOHO is a mission of international cooperation between ESA and NASA. The SUMER project is financially supported by DLR, CNES, NASA and ESA PRODEX programme (Swiss contribution). We thank the EIT team for the use of the He I 30.4 nm images to determine the scattered light contribution. We acknowledge the use of SOLSTICE and TIMED/SEE data obtained from the web page `lasp.colorado.edu/lisird`. We thank the referee and the editor for helpful comments.

## Appendix A: Observation parameters

For each observation (either Ly-$\alpha$ or Ly-$\beta$, see Table A.1 and Table A.2) we provide:

- the time of the beginning of the observation. The duration of each observation (multiple exposures) at the same $X$ and $Y$ location was four hours to accumulate enough counts well above the detector noise. (The detector noise is less than 1.e-4 count per second per pixel). When there are four slit locations, the duration at each location is limited to 2 h;
- the slit location measured from the solar disc centre ($X$ and $Y$ axes) at the time of observation;
- the detector (A or B) selected;
- the Ly-$\alpha$ irradiance of the day provided by *composite_lya.dat* from lasp.colorado.edu/lisird;

**Table A.1.** Ly-$\alpha$ observations.

| Starting time | Slit location | Detector | Ly-$\alpha$ irradiance | $F_{10.7}$ |
|---|---|---|---|---|
| year/month/day hr:mn | $X, Y$ | | $10^{11}$ | $10^{-22}$ |
| | arcsec | | ph cm$^{-2}$ s$^{-1}$ | W m$^{-2}$ Hz$^{-1}$ |
| 1996/05/26 19 :23 | ±1200, ±1500 | A | 3.53 | 68.7 |
| 1996/06/10 00 :02 | ±1200, ±1500 | A | 3.59 | 71.1 |
| 1996/07/27 03 :14 | ±1200, ±1500 | A | 3.65 | 75.6 |
| 1996/09/15 19 :32 | ±1200, ±1500 | A | 3.53 | 67.1 |
| 1996/10/28 17 :08 | 0, ±1700 | B | 3.54 | 67.5 |
| 1996/11/26 08 :48 | 0, ±1700 | B | 3.64 | 100.8 |
| 1996/12/05 04 :14 | 0, −1700 | B | 3.55 | 67.6 |
| 1996/12/05 11 :02 | 0, −1700 | B | 3.55 | 67.6 |
| 1997/02/17 15 :42 | 0, ±1700 | B | 3.54 | 71.4 |
| 1997/05/22 23 :17 | 650, ±1700 | B | 3.65 | 83.0 |
| 1997/08/22 22 :31 | 0, +1400 | B | 3.61 | 77.2 |
| 1997/08/24 22 :32 | 0, ±1700 | B | 3.63 | 79.4 |
| 1997/08/26 22 :01 | 600, +1100 | B | 3.68 | 85.5 |
| 1997/12/02 05 :01 | 0, ±1700 | B | 4.21 | 109.0 |
| 1997/12/04 13 :06 | 0, ±1700 | B | 4.05 | 101.1 |
| 1997/12/06 00 :04 | 0, ±1700 | B | 3.97 | 105.6 |
| 1997/12/10 00 :03 | 0, ±1700 | B | 3.87 | 92.2 |
| 1997/12/13 00 :04 | 0, ±1700 | B | 3.82 | 86.5 |
| 1997/08/24 22 :32 | 0, ±1700 | B | 3.62 | 79.4 |
| 1998/02/19 00 :08 | 0, ±1700 | B | 4.05 | 96.3 |
| 1998/06/08 21 :01 | 0, ±1700 | B | 4.30 | 120.6 |
| 1999/03/13 22 :01 | 0, ±1700 | A | 4.83 | 142.7 |
| 1999/08/20 20 :22 | 0, ±1700 | B | 4.73 | 165.0 |
| 2000/05/20 00 :06 | −290, ±1700 | A | 5.55 | 251.6 |
| 2000/11/12 16 :01 | −1000, ±1700 | A | 5.02 | 143.6 |
| 2001/03/26 09 :05 | 954, ±1437 | A | 5.75 | 262.6 |
| 2001/08/22 00 :33 | 860, ±1700 | A | 5.28 | 165.2 |
| 2001/08/24 17 :03 | 860, +1700 | A | 5.38 | 178.7 |
| 2001/08/27 10 :08 | 860, −1700 | A | 5.49 | 195.9 |
| 2001/10/28 13 :02 | 0, ±1700 | A | 5.85 | 224.2 |
| 2002/05/23 20 :32 | 965, ±1437 | A | 5.31 | 154.8 |
| 2002/08/22 01 :00 | 0, ±1700 | A | 5.66 | 225.0 |
| 2002/10/23 06 :01 | 0, ±1700 | A | 5.13 | 161.9 |
| 2003/05/29 01 :01 | 650, ±1600 | A | 4.76 | 141.0 |
| 2003/08/24 03 :03 | 0, ±1700 | A | 4.66 | 119.0 |
| 2003/11/27 08 :52 | 1060, ±1600 | A | 5.06 | 170.1 |
| 2004/06/05 10 :42 | 886, ±1600 | A | 4.22 | 87.0 |
| 2007/03/27 01 :40 | 860, ±1700 | B | 3.70 | 73.0 |
| 2007/11/01 00 :01 | 0, ±1700 | B | 3.49 | 66.3 |
| 2008/04/04 23 :31 | 0, ±1700 | B | 3.59 | 73.1 |
| 2008/09/20 02 :01 | 0, ±1700 | B | 3.47 | 68.4 |
| 2008/09/23 10 :55 | 0, ±1700 | B | 3.52 | 69.8 |
| 2008/10/04 01 :01 | 0, ±1700 | B | 3.47 | 66.6 |
| 2009/04/16 01 :00 | 860, ±1700 | B | 3.50 | 70.5 |

**Notes.** The Ly-$\alpha$ irradiance values are taken from *composite_lya.dat* (lasp.colorado.edu/lisird, Woods et al. 2000), and the $F_{10.7}$ values are taken from *Solar Indices Bulletin* (National Geophysical Data Center, STP Division).

**Table A.2.** Ly-$\beta$ observations.

| Starting time | Slit location | Detector | Ly-$\alpha$ irradiance | $F_{10.7}$ |
|---|---|---|---|---|
| year/month/day hr:mn | $X, Y$ | | $10^{11}$ | $10^{-22}$ |
| | arcsec | | ph cm$^{-2}$ s$^{-1}$ | W m$^{-2}$ Hz$^{-1}$ |
| 1996/07/19 22 :11 | ±1200, ±1500 | A | 3.50 | 68.3 |
| 1996/10/07 01 :01 | ±1200, ±1500 | B | 3.49 | 68.2 |
| 1996/10/29 21 :04 | 0, ±1700 | B | 3.50 | 69.4 |
| 1996/11/27 08 :04 | 0, ±1700 | B | 3.62 | 100.0 |
| 1997/03/28 01 :02 | 0, ±1700 | B | 72.9 | 3.56 |
| 1997/05/25 22 :11 | 640, +1000 | B | 3.67 | 80.1 |
| 1997/08/23 07 :00 | 0, +1300 | B | 3.62 | 78.2 |
| 1997/08/24 08 :31 | 0, ±1700 | B | 3.63 | 79.4 |
| 1997/12/03 10 :31 | 0, ±1700 | B | 4.14 | 109.0 |
| 1997/12/04 05 :01 | 0, +1200 | B | 4.05 | 101.2 |
| 1997/12/13 16 :02 | 0, ±1700 | B | 3.82 | 86.5 |
| 1998/02/20 00 :08 | 0, ±1700 | B | 4.05 | 83.8 |
| 1998/06/09 20 :01 | 0, ±1700 | B | 4.30 | 115.7 |
| 1999/03/14 05 :43 | 0, ±1700 | A | 4.89 | 148.7 |
| 1999/08/21 06 :06 | 0, ±1700 | B | 4.73 | 165.0 |
| 2000/05/21 00 :03 | −290, ±1700 | A | 5.44 | 238.0 |
| 2000/11/07 01 :01 | −1000, ±1700 | A | 5.42 | 176.6 |
| 2001/05/14 20 :31 | 862, +1700 | A | 4.99 | 141.2 |
| 2001/05/21 20 :07 | 860, +1429 | A | 5.07 | 153.8 |
| 2001/05/22 04 :22 | 860, +1630 | A | 5.08 | 155.8 |
| 2001/08/22 08 :30 | 860, ±1700 | A | 5.28 | 165.2 |
| 2001/10/29 00 :03 | 0, ±1700 | A | 5.78 | 212.8 |
| 2002/05/24 15 :01 | 950, ±1700 | A | 5.36 | 193.9 |
| 2002/05/29 00 :01 | 0, +1415 | A | 5.31 | 189.8 |
| 2002/05/29 04 :01 | 0, +1685 | A | 5.31 | 189.8 |
| 2002/05/31 02 :01 | 0, +1415 | A | 5.29 | 187.0 |
| 2002/05/31 06 :01 | 0, +1685 | A | 5.29 | 187.0 |
| 2002/08/22 08 :54 | 0, ±1700 | A | 5.66 | 225.1 |
| 2002/10/24 06 :01 | 0, +1700 | A | 5.10 | 158.5 |
| 2003/05/25 09 :35 | 0, ±1700 | A | 4.84 | 124.3 |
| 2003/08/24 16 :00 | 0, ±1700 | A | 4.66 | 119.0 |
| 2003/11/21 10 :02 | 0, ±1700 | A | 4.85 | 172.8 |
| 2004/06/05 18 :46 | 886, ±1700 | A | 4.22 | 91.0 |
| 2007/03/27 09 :33 | 950, ±1700 | B | 3.70 | 73.0 |
| 2008/04/04 07 :04 | 0, ±1700 | B | 3.59 | 73.1 |
| 2008/09/20 16 :36 | 0, +1700 | B | 3.47 | 68.4 |
| 2008/09/23 03 :12 | 0, ±1700 | B | 3.52 | 69.8 |
| 2008/10/04 16 :00 | 0, ±1700 | B | 3.47 | 66.6 |
| 2009/04/16 12 :30 | 950, ±1700 | B | 3.50 | 70.5 |

**Notes.** The Ly-$\alpha$ irradiance values are taken from *composite_lya.dat* (http://lasp.colorado.edu/lisird, Woods et al. 2000) and the $F_{10.7}$ values from *Solar Indices Bulletin* (National Geophysical Data Center, STP Division).

– the 10.7 cm solar flux ($F_{10.7}$) of the day given in the *Solar indices Bulletin* (National Geophysical Data Center, STP Division).

## References


Auchère, F. 2005, ApJ, 622, 737

Barthélémy, M., Parkinson, C., Lilensten, J., & Prangé, R. 2004, A&A, 423, 391

Bertaux, J.-L., Blamont, J.-E., & Festou, M. 1973, A&A, 25, 415

Bertaux, J. L., Combi, M. R., Quémerais, E., & Schmidt, W. 2014, Planet. Space Sci., 91, 14

Bourrier, V., Lecavelier des Etangs, A., Dupuy, H., et al. 2013, A&A, 579, A63

Bzowski, M., Sokół, J. M., Tokumaru, M., et al. 2013, in Cross-Calibration of the Far UV Spectra of Solar System Objects and the Heliosphere, eds. E. Quémerais, M. Snow, & R. M. Bonnet, Bern, ISSI SR-013, 67

Curdt, W., & Tian, H. 2010, in SOHO-23: Understanding a Pecular Solar Minimum, eds. S. R. Cranmer, J. T. Hoeksema, & J. L. Kohl, ASP Conf. Ser., 428, 81

Delaboudinière, J.-P., Artzner, G. E., Brunaud, J., et al. 1995, Sol. Phys., 162, 291

Ebadi, H., Vial, J.-C., & Ajabshirizadeh 2009, Sol. Phys., 257, 91

Emerich, C., Ben Jaffel, L., Clarke, J. T., & Ballester, G. 2005, in Highlights of Astronomy, ed O. Engvold, IAU 2003, 13, 917

Emerich, C.,Lemaire, P., Vial, J.-C., et al. 2005, Icarus, 178, 429

Feldman, P. D., Opal, C. B., Meier, R. R., & Nicolas, K. R. 1976, NASA SP, 393, 773

Haisch, B. M., Linsky, J. L., Weinstein, A., & Shine, R. A. 1977, ApJ, 214, 785
Lemaire, P. 2002, in The Radiometric Calibration of SOHO, eds. A. Pauluhn, M. C. E. Huber, & R. von Steiger, ISSI SR-002, 265
Lemaire, P., Charra, J., Jouchoux, A., et al. 1978, ApJ, 223, L55
Lemaire, P., Wilhelm, K., Curdt, W., et al. 1997, Sol. Phys., 170, 105
Lemaire, P., Emerich, C., Curdt, W., Schühle, U., & Wilhelm, K. 1998, A&A, 334, 1095
Lemaire, P., Emerich, C., Vial, J.-C., et al. 2002, in From Solar Min to Max: half a Solar Cycle with SOHO, ed. A. Wilson, ESA SP, 508, 219
Lemaire, P., Emerich, C., Vial, J.-C., et al. 2005, Adv. Space Res., 35, 384
Lemaire, P., Vial, J.-C., Curdt, W., Schühle, U., & Woods, T. N. 2012, A&A, 542, L25
Miguel, Y., Kaltenegger, L., Linsky, J. L., & Rugheimer, S. 2015, MNRAS, 446, 345
Nina, A., & Cadez, V. M. 1978, Adv. Space Res., 54, 1276
Nichols, J. D., Bunce, E. J., Clarke, J. T., et al. 2007, J. Geophys. Res., 112, 2203
Saha, T. T., Leviton, D. B., & Glenn, P. 1996, Appl. Opt., 35, 1742
Tian, H., Curdt, W., Marsch, E., & Schühle, U. 2009, A&A, 504, 239
Vernazza, J. E., & Reeves, E. M. 1978, ApJ, 37, 485
Vial, J.-C., Eurin, G., & Curdt, W. 2015, Sol. Phys., 290, 381
Vidal-Madjar, A. 1975, Sol. Phys., 40, 69
Waniak, W. 1997, A&AS, 124, 197
Wilhelm, K., Curdt, W., Marsch, E., et al. 1995, Sol. Phys., 162, 189
Wilhelm, K., Lemaire, P., Curdt, W., et al. 1997, Sol. Phys., 170, 75
Woods, T. N., Tobiska, W. K., Rottman, G. J., & Worden, J. R. 2000, J. Geophys. Res., 105, 27217
Woods, T. N., Eparvier, F. G., Bailey, S. M., et al. 2005, J. Geophys. Res., 110, A01312